PET/CT of Tumors of the Ear and Temporal Bone

16

Guoren Yang, Zhenguang Wang, Dacheng Li, and Tingting Lu

1 Overview

Ear tumors can be classified into tumors of the external ear and external auditory canal, middle ear, and internal ear.

Tumors of the external ear and external auditory canal may originate from various tissues including the bone, cartilage, blood vessels, skin, glands, etc., most of which are benign. Common tumors include osteomas, papillomas, fibromas, ceruminous adenomas, hemangiomas, etc. Clinical symptoms are generally not obvious, and when the tumor is large and exerts compression or obstruction on the external auditory canal, the affected side is inflicted with hearing loss, infection in the external auditory canal, and other manifestations. Malignant tumors are rare, most of which are metastatic. The primary malignant tumors are squamous cell carcinoma, and other types of tumors include basal cell carcinoma, adenoid cystic carcinoma, ceruminous gland adenocarcinoma, etc. Clinical manifestations include earache, hearing loss, discharge of pus and bleeding, facial paralysis, etc. The external ear and external auditory canal are shallow and exposed, and polypoid or cauliflower-like masses of the external auditory canal can be easily found by physical examination. Obtaining pathological diagnosis is the main means of diagnosis, and imaging including PET/CT examination is mainly intended to determine the range and understanding whether there is metastasis.

Tumors of the middle ear are rare, and the middle ear is deep and hidden, so it is difficult to obtain pathological diagnosis. Most malignancies of the middle ear are secondary to or associated with inflammation and are often diagnosed late because of the confusion between the two. Common benign tumors of the middle ear include facial neuroma and glomus tumors of the tympanic cavity. Carcinoma of the middle ear accounts for 1.5% of the tumors of the ear, of which squamous cell carcinoma is the most common type with high degree of malignancy, followed by basal cell carcinoma, adenocarcinoma, and metastatic tumor which are rare. Primary tumors of the external ear, nasopharynx, and so on can invade the middle ear, and it is often difficult to determine the primary site on imaging.

The vast majority of ear tumors occur in the external and middle ear, but very few occur in the internal ear. The overwhelming majority of tumors in the labyrinth and internal auditory canal are schwannomas, which can originate from the vestibular nerve, cochlear nerve, and facial nerve, most of which originate from the vestibular nerve. Schwannomas in the internal auditory canal are more common than those in the labyrinth. Most of them are unilateral, while a few can be bilateral, which is called type II neurofibromatosis.

2 Osteoma of the Ear

2.1 Clinical Overview

Osteoma is a benign bone tumor originating from the periosteum tissue, which usually occurs on the bone wall of the skull, maxilla, mandible, and sinuses and is rarely seen in the ear. Auricular osteoma can be seen in the external auditory

G. Yang (✉) · T. Lu
Shandong Cancer Hospital, Jinan, Shandong, China

Z. Wang · D. Li
The Affiliated Hospital of Qingdao University, Qingdao, Shandong, China

Z. Yao, S. Li (eds.), *Atlas of PET/CT in Oncology - Volume 1*, https://doi.org/10.1007/978-981-99-1172-1_16

canal, mastoid process, tympanic cavity, squamous part of the temporal bone, etc., among which the external auditory canal and mastoid process are more inflicted. Osteomas can be classified into dense type and loose type. Osteomas of the external auditory canal are of mostly dense type, which are usually unilateral and single, and grow slowly.

2.2 PET/CT Diagnostic Points

CT images show spherical or hemispherical bone density nodules and masses in the osseous parts of the external auditory canal, with prominent protruding toward inside the external auditory canal cavity, characterized with regular and smooth surfaces. It has pedicle and is connected with the bone wall of the external auditory canal, and a few are with broad base. They are mostly unilateral occurrence and grow singly.

^{18}F-FDG PET image showed no metabolic activity in lesions.

2.3 Typical Cases

The patient, a 45-year-old male, was present due to "occupancy of the external auditory canal found by this examination" (Fig. 16.1).

2.4 Summary

Since there was no abnormal metabolic activity of ear osteoma, this disease was not an indication of FDG PET/CT and was usually diagnosed by CT.

3 Malignant Tumor of the External Auditory Canal

3.1 Clinical Overview

The reason of malignant tumor of the external auditory canal is not known, and it is mostly related to injury, chronic inflammation, and fungal infection of the external auditory canal. Squamous cell carcinoma is the most common pathological type, followed by adenoid cystic carcinoma. Early carcinoma of the external auditory canal often does not have subjective symptom, can show only for slight pruritus or ache, and is not easy to discover. The lesion progression may involve cartilage or bone, with persistent severe earache and radiating to the ipsilateral temporal, shoulder, and occipital regions. When accompanied with infection, it can be inflicted with discharge of pus and stream fluid in the ear, and advanced tumor can invade the middle ear and parotid gland and even invade into the skull upward.

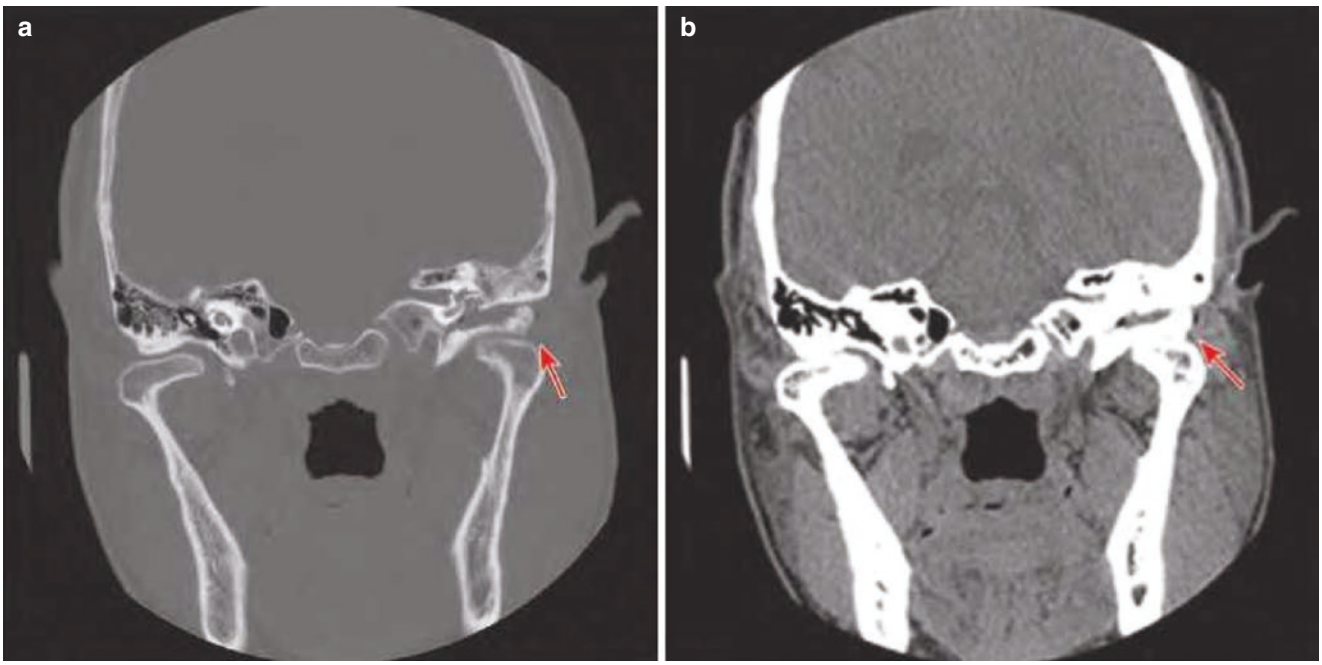

Fig. 16.1 CT images of osteoma in the external auditory canal. (**a**) Coronal CT bone window image. (**b**) Coronal CT soft tissue window image. The arrow in the figure shows the bone density nodules of the left external auditory canal, protruding into the cavity of the external auditory canal, with a slightly wider base connected to the bone wall of the external auditory canal, with neat and smooth edges

Tumors of the external auditory canal are easily pathologically diagnosed. Imaging methods, including PET/CT, are mainly used to determine the primary site and lesion invasion scope and to understand the metastasis, which are of reference value for guiding biopsy, surgical selection, and postoperative comprehensive treatment. The imaging findings of malignant tumors of the external auditory canal of different pathological types are not specific.

3.2 PET/CT Diagnostic Points

1. The external auditory canal is filled with density shadow of soft tissue, and the external auditory canal is damaged by bone. Bone destruction, invasion of surrounding structures, and edema of surrounding soft tissues are the main bases for CT to judge malignant lesions of the external auditory canal.
2. The lesion progresses and invades in all directions; the lesion can invade the middle ear and mastoid process to the medial side, the skull base, and the skull and invade the parotid gland outward.
3. ^{18}F-FDG PET shows increased metabolism of tumors in the external auditory canal, which helps to determine the extent of invasion of surrounding structures, cervical lymph node metastasis, and distant metastasis.

3.3 Typical Cases

The patient was a 49-year-old female with left ear discomfort for 1 month (Fig. 16.2).

Follow-up ^{18}F-FDG PET/CT after surgical operation 6 months for a poorly differentiated nonspecific adenocarcinoma of the left external auditory canal (Fig. 16.3)

Follow-up ^{18}F-FDG PET/CT after surgical operation 8 months for squamous carcinoma of the left external auditory canal; she was reexamined with ^{18}F-FDG PET/CT (Fig. 16.4).

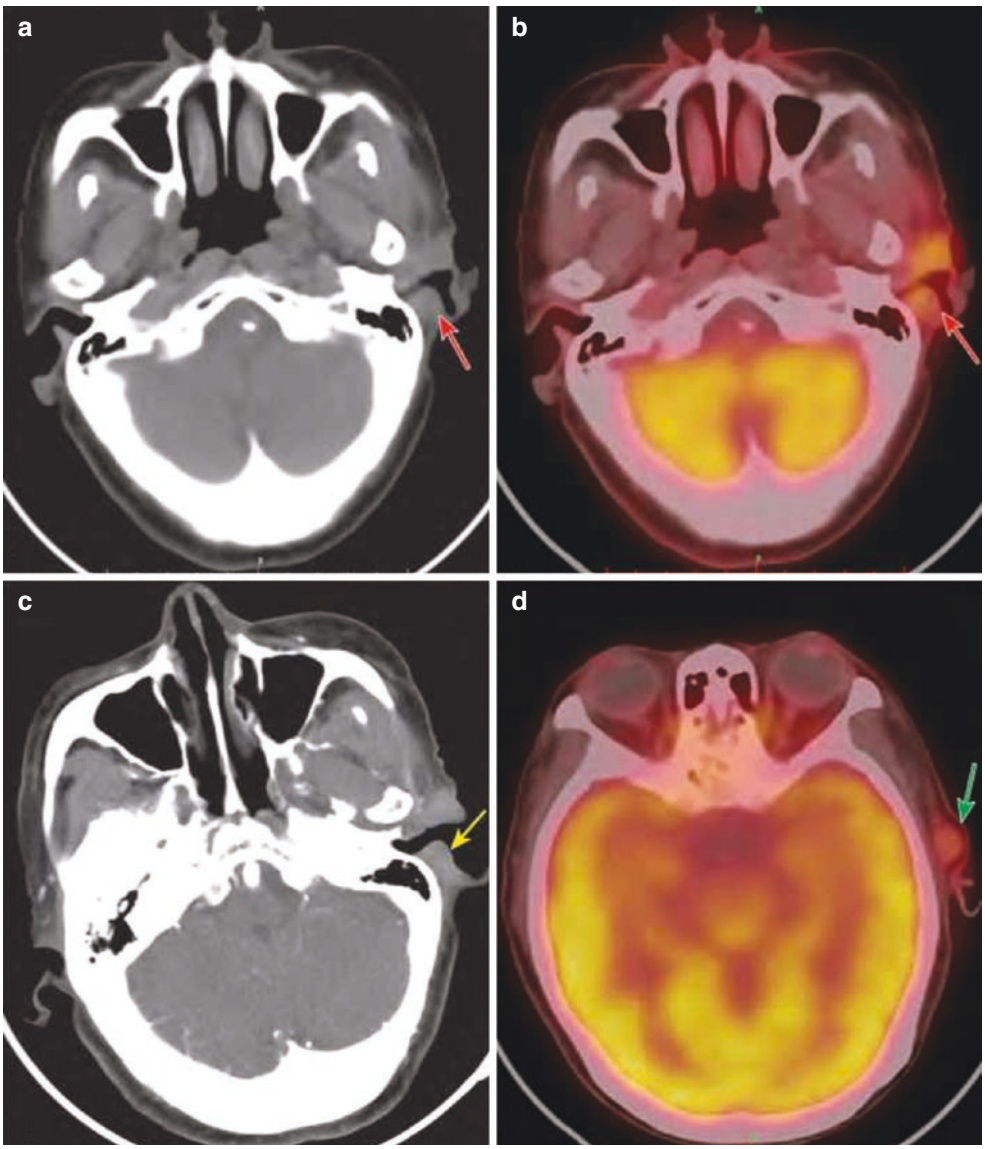

Fig. 16.2 ^{18}F-FDG PET/CT and enhanced CT images of basal cell carcinoma of the external auditory canal. (**a**) CT image. (**b**) ^{18}F-FDG PET/CT fusion image showed the soft tissue of the left external auditory canal was significantly thickened and hypermetabolic (red arrow) with SUVmax 7.1. (**c**) Enhanced CT images showed obvious enhancement of soft tissue lesions in the left external auditory canal (yellow arrow). (**d**) ^{18}F-FDG PET/CT fusion image showed enlarged lymph nodes in front of the left ear with increased metabolism and SUVmax of about 3.8, which was considered as lymph node metastasis (green arrow). It was confirmed through pathology with basal cell carcinoma of the left external auditory canal

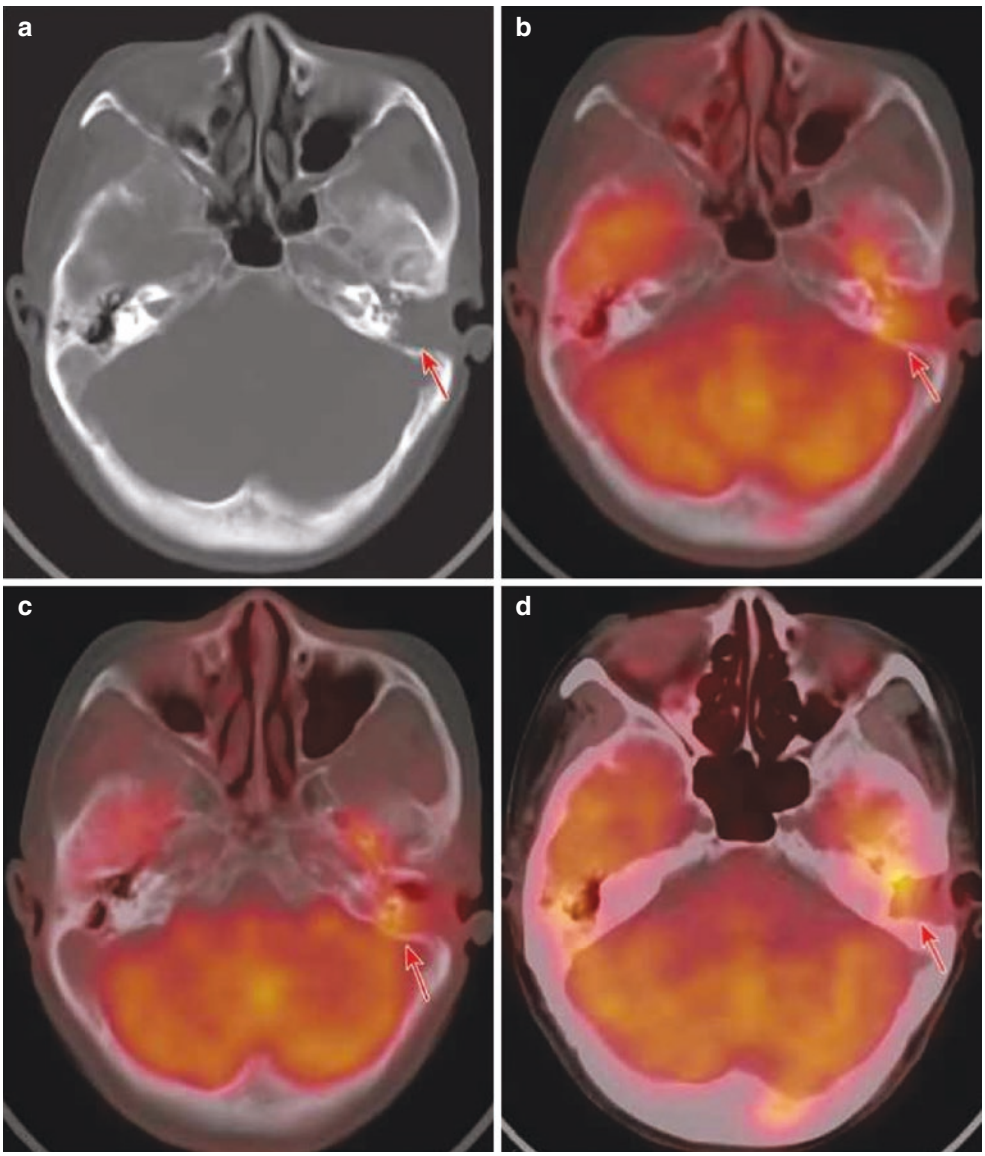

Fig. 16.3 ^{18}F-FDG PET/CT images of recurrent adenocarcinoma of the external auditory canal after resection. (**a**) CT bone window image, bone absence in the left posterior wall of the external auditory canal and the left mastoid part of the temporal bone; soft tissue density lesions were seen in the left external and middle ear canal, and the surrounding bone showed bone destruction like worm erosion, with lesions invading the petrous part of the temporal bone. (**b, c**) Bone window fusion images. (**d**) Window fusion image of soft tissue showed significantly increased metabolism in soft tissue lesion and surrounding bone destruction area, with SUVmax 8.7, and lesions invading the skull base in front and above. Pathology confirmed recurrence

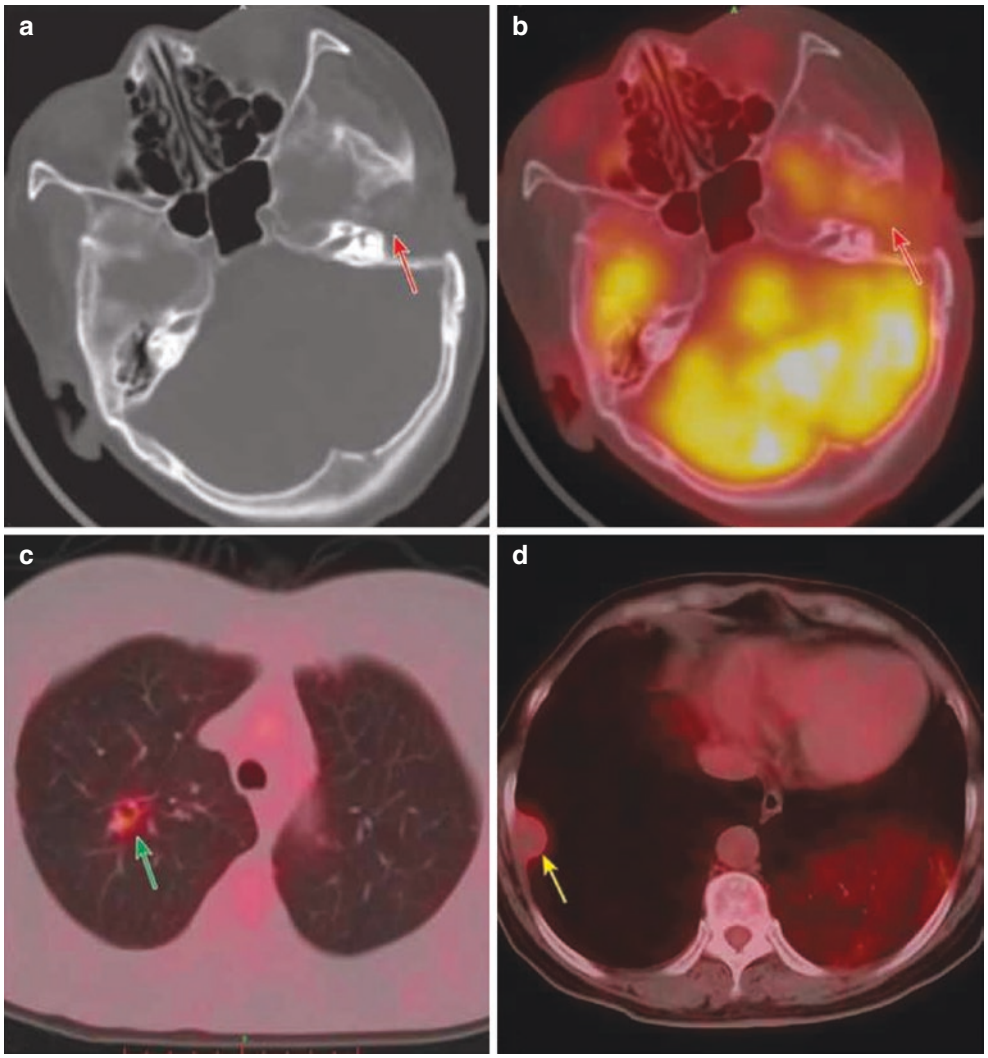

Fig. 16.4 ^{18}F-FDG PET/CT images of recurrence and metastasis occurred after resection of squamous cell carcinoma of the external auditory canal. (**a**) CT image of bone window of the left external auditory canal: bone of the left posterior wall of the external auditory canal and the left mastoid part of the left temporal bone was absent, and the anterior bone of the operative area was seen with destruction like worm-eaten shape. (**b**) PET/CT fusion image of the left external auditory canal: the lesions in the above left external auditory canal showed increased metabolism, with SUVmax 4.3 (red arrow). (**c**) Lung PET/CT fusion image: increased metabolism (SUVmax 3.2) in the cavitary nodules in the upper lobe of the right lung. (**d**) Chest PET/CT fusion image: right pleural nodules with increased metabolism and SUVmax 2.7. The diagnosis with ^{18}F-FDG PET/CT image showed recurrence with pulmonary metastasis (green arrow) and right pleural metastasis (yellow arrow). A puncture biopsy of the right pleural nodule showed infiltration of highly differentiated squamous cell carcinoma in the proliferative fibrous adipose tissue, which was considered to be metastatic based on the medical history

3.4 Differential Diagnosis

Granulation tissue: Granulation tissue is usually secondary to other diseases such as inflammation, trauma, surgery, etc. In most cases, there is no peripheral bone damage, or the damage is mild. Inflammation of the external auditory canal is easy to be diagnosed. There is no soft tissue mass formation (Figs. 16.5 and 16.6).

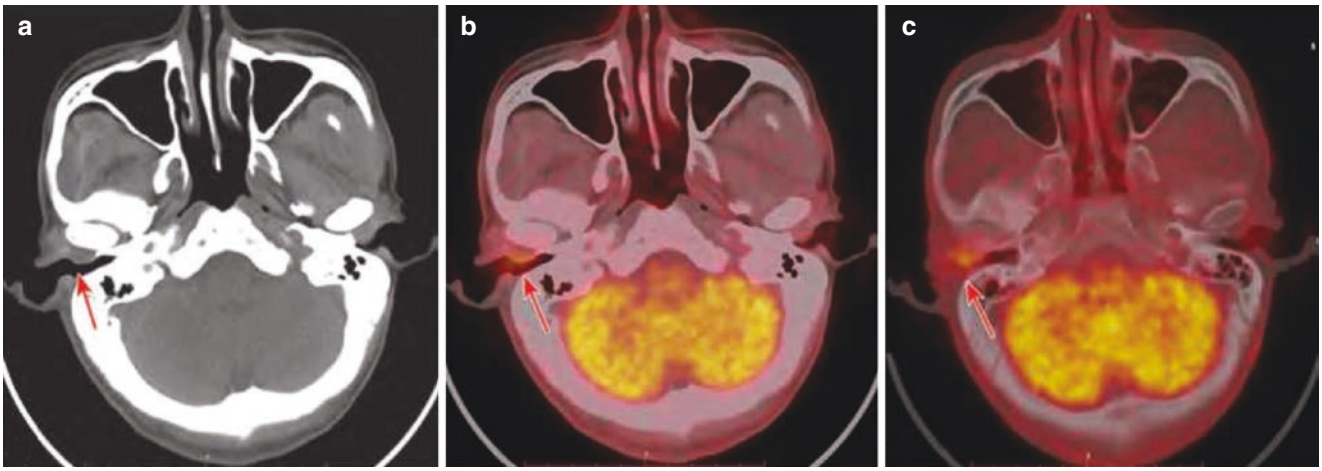

Fig. 16.5 ^{18}F-FDG PET/CT images of otitis externa. (**a**) CT image (soft tissue window) showed slight thickening of soft tissue in the anterior wall of the right external auditory canal with smooth edges. (**b**) PET/CT fusion image (soft tissue window) showed mild increased local metabolism, with SUVmax of 4.4. (**c**) PET/CT fusion image (bone window) showed no adjacent bone destruction and erosion. The patient was effectively treated with antibiotics

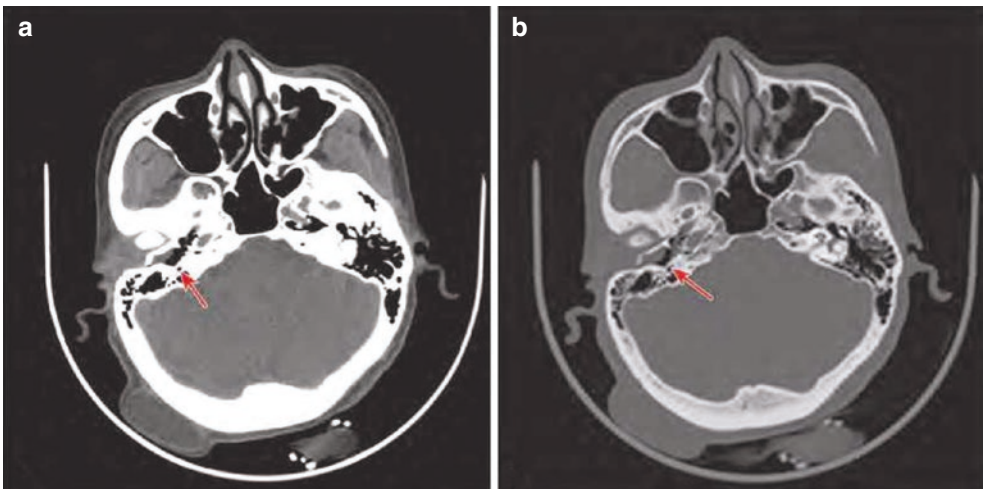

Fig. 16.6 CT images of fungal infection of the external auditory canal and middle ear. (**a**) CT soft tissue window image. (**b**) CT bone window image. The arrow in the figure showed the right external auditory meatus—tympanic cavity had soft striate tissue density shadow with smooth edges and without adjacent bone erosion. Pathology: There was a little keratinized substance under the microscope (in the right external auditory canal tissue), and the fungal spore-like structure was found inside, which was consistent with fungal infection. Hexamine silver (+)

3.5 Summary

The external auditory canal tumors with hypermetabolic activity are easily confused with infectious diseases of the external auditory canal.

4 Carcinoma of the Middle Ear

4.1 Clinical Overview

Carcinoma of the middle ear is more common in middle-aged and elderly patients. The majority of the cases were pathologically squamous cell carcinomas arising from the mucosae epithelium of the middle ear cavity. Due to the inter-connection of the tympanic cavity, tympanic sinus, mastoid air chamber, pharyngotympanic tube, and other parts, malignant tumors of the middle ear are easy to spread to the inferior tympanic cavity, perilabyrinth, and mastoid air chamber, and often have obvious damage to the adjacent bone, and can also invade the petrous apex, parotid gland, and temporomandibular joint. Next is sarcoma, which is associated with local radiation exposure, trauma, viral infection, and malignant transformation of some benign tumors, and it develops rapidly and may have early distant metastases. Adenocarcinoma of the middle ear is rare and originates from the mucous gland of the mucosa of the tympanic membrane, which grows slowly and can have local invasion and exert damage.

About 80%–85% of patients with carcinoma of the middle ear have a history of chronic suppurative otitis media, so there are no characteristic clinical symptoms, and in addition to long-term chronic mastoiditis manifestations of the middle ear, the patient may suffer from bleeding, pus, and severe pain in the auditory canal, facial paralysis, etc.

4.2 PET/CT Diagnostic Points

1. Soft tissue density mass in the middle ear cavity, invading the surrounding tissues with the tympanic cavity as the center, can invade the external auditory canal, pharyngotympanic tube, internal ear, mastoid sinus, mastoid process, etc. and even invade the parotid gland, inferior temporal fossa, and intracranial part.
2. There is extensive and obvious bone damage; the edge of the damaged lesion is of worm-eaten shape and irregular; the ossicle is damaged; moderate or significant enhancement is seen.
3. ^{18}F-FDG PET shows increased metabolism in the lesion. PET/CT can be used to determine the lesion invasion scope, metastasis of cervical lymph node, and distant metastasis and is also of help to determine whether it is a direct invasion to the middle ear, such as nasopharyngeal carcinoma.

4.3 Typical Cases

The patient, a 41-year old male, was present 3 months after surgery for adenoid cystic carcinoma of the right tympanic cavity, with right earache for 1 month and with drooping of the angle of the mouth over 1 week (Fig. 16.7).

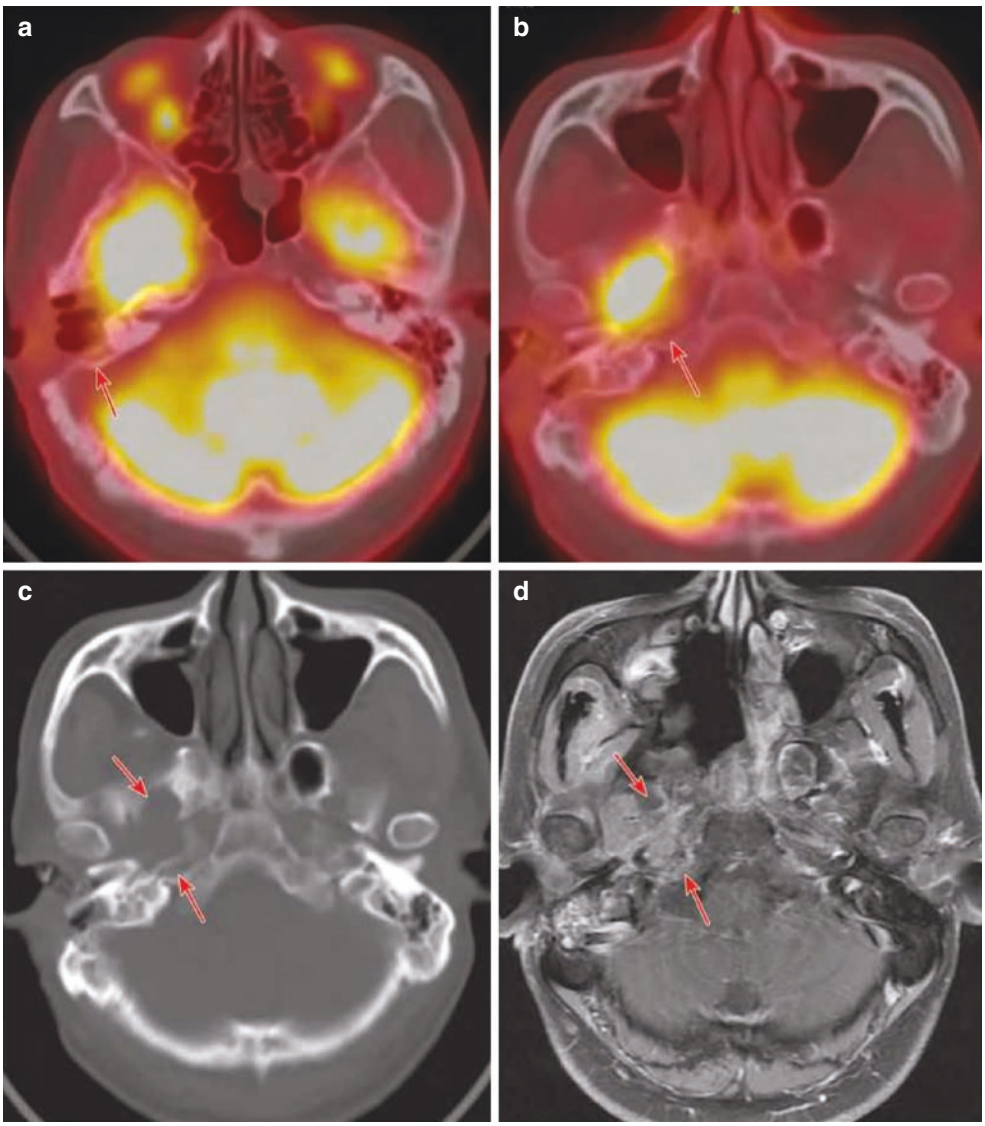

Fig. 16.7 ^{18}F-FDG PET/CT images showing local invasion after surgery for adenoid cystic carcinoma of the tympanic cavity of the middle ear. (**a**) PET/CT cross section of fusion image at the level of the right tympanic cavity: Bone loss was found in the bone wall around the right tympanic cavity and in the right mastoid part, and no abnormal increase in metabolism was observed locally. (**b, c**) PET/CT fusion image and CT window image of the right temporal bone, respectively: osteolytic bone destruction was observed in the petrous apex of the right temporal bone, the pterygoid process and the greater wing of sphenoid bone. A soft tissue mass was noted with increased metabolism (SUVmax12.2). (**d**) Enhanced MR image of the right temporal bone: irregular morphology of the damaged area showed moderate heterogeneous enhancement. The patient had a local invasion after middle ear carcinoma

4.4 Differential Diagnosis

1. Congenital cholesteatoma It more commonly occurs in the superior tympanic cavity, with regular margins and clear masses, which may be accompanied by erosion of the middle ear wall or loss of the ossicle.
2. Glomus tympanicum tumor There are density nodes in the promontory and the surrounding soft tissues, mostly without obvious bone destruction.

5 Metastatic Tumor of the Temporal Bone

5.1 Clinical Overview

Metastatic tumors of the temporal bone are rare and most common in the elderly. There are three main routes:

1. Hematogenous metastasis: The temporal bone is rich in bone marrow and blood supply, and primary tumors in other areas can be transferred to the temporal bone through blood flow, among which breast cancer is the most common, followed by lung cancer, kidney cancer, prostate cancer, melanoma, etc.
2. Lymphatic metastasis: Upper respiratory tract and digestive tract tumors have been reported to invade the temporal bone through the retropharyngeal lymph nodes.
3. Direct invasion: The adjacent relationship around the temporal bone is complicated, and tumors with multiple channels communicating with adjacent structures can directly invade the temporal bone, such as nasopharyngeal carcinoma and parotid malignant tumor. The clinical manifestations of temporal bone metastases include headache, abducent nerve paralysis, hearing loss, etc., and imaging findings are not specific.

5.2 PET/CT Diagnostic Points

1. CT findings are varied and associated with the biological behavior and pathological type of primary cancer. The metastatic tumors to the nose are mainly osteolytic bone destruction and rarely osteogenic one. Bone metastasis of breast cancer is mostly osteolytic, mainly manifested as worm-biting-like or rat-biting-like irregular bone destruction, with or without soft tissue density mass. In lung cancer, bone metastasis usually occurs in adenocarcinoma, mainly with osteolytic bone destruction. Small cell undifferentiated carcinoma and a few adenocarcinoma can present osteoblastic metastasis. The majority of renal carcinoma is osteolytic metastasis. Osteoblastic metastases may resemble benign fibrous bone disease.
2. ^{18}F-FDG PET/CT findings of bone metastases mostly show increased metabolic manifestations, and the degree of metabolism increase depends on the pathological type and metabolic level of primary tumor and the type of local bone destruction. The metabolic activity of osteolytic bone metastasis was increased significantly, while that of osteogenic bone metastasis was slightly higher or even without increase. The osteogenic changes of the temporal bone can be detected by CT, and the osteogenic metastasis of the temporal bone can be diagnosed by combining with lesion's metabolic activity.
3. Single bone metastasis in patient is rare; most are multiple bone metastases. ^{18}F-FDG PET/CT is a systemic examination, which is of great value in the detection of the metastasis in the whole body and understanding well the primary lesion. The discovery of bone metastases in other locations of body is very helpful in improving the diagnostic confidence of bone metastases in the temporal bone.

5.3 Typical Cases

Case 1: A 55-year-old female patient with a right breast mass for 10 months and a headache for 2 months. Pathology: (Biopsy of the right breast) Poorly differentiated invasive carcinoma (Fig. 16.8)

Case 2: Male patient, 66 years old. Due to headache, bone destruction was found in the petrous part of the left temporal bone. PET/CT examination was requested to find out the primary lesion. Pathology: Medium differentiation adenocarcinoma in the upper lobe of the right lung with metastasis to the petrous part of the left temporal bone and sacrum (Fig. 16.9)

Case 3: Male patient, 52 years old. 7 years after surgery for atypical carcinoid tumors of the thymus. Bone metastasis was found for 1 year, and octreotide was used for treatment for 1 year. PET/CT examination was applied to understand the recurrence and metastasis (Fig. 16.10).

Case 4: A typical case photo of poorly differentiated squamous cell carcinoma of the left pharyngeal recess (Fig. 16.11)

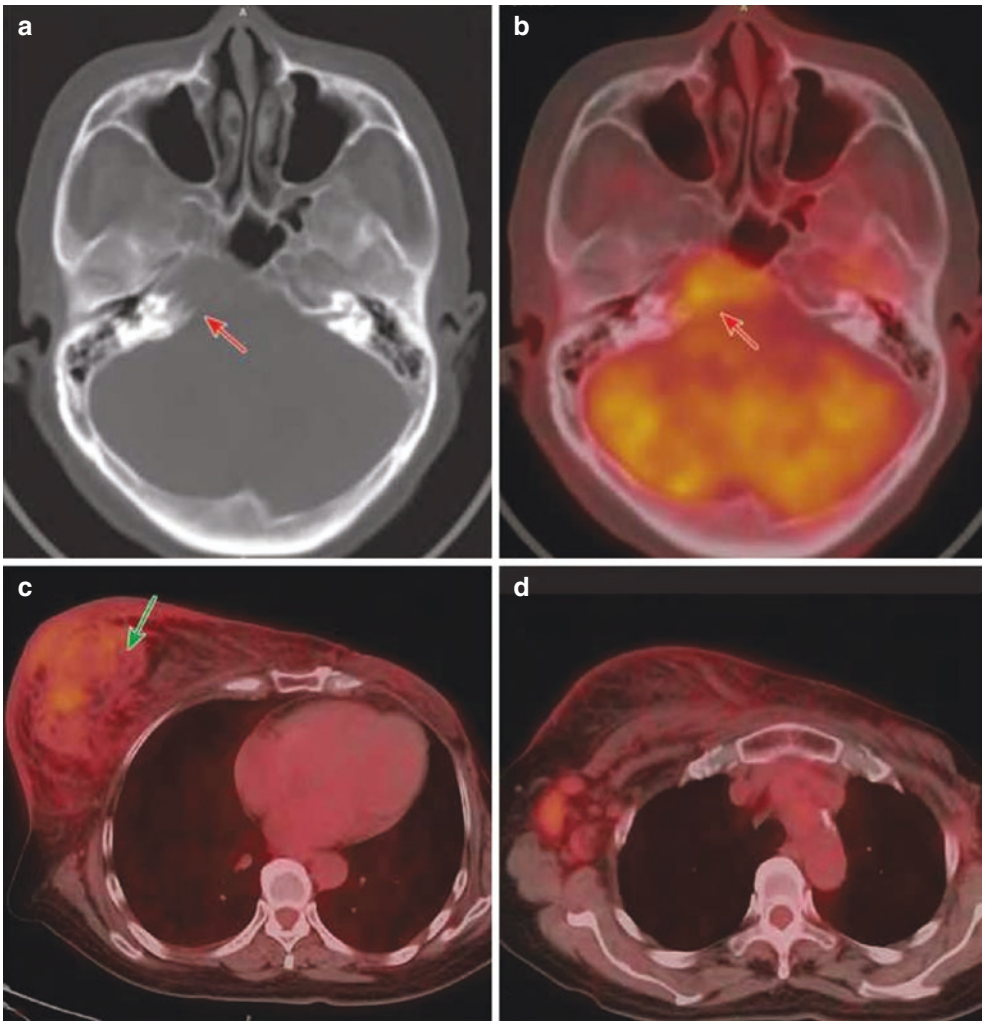

Fig. 16.8 ^{18}F-FDG PET/CT image of metastases of the petrous apex of the temporal bone. (**a** and **b**) CT bone window image and cross section of PET/CT fusion image of the temporal bone, respectively: CT showed osteolysis bone destruction at the petrous apex of the right temporal bone, with irregular edges of the lesion destroyed; PET/CT fusion image showed increased metabolism in bone destruction lesion, with SUVmax of about 5.0. (**c**) Breast PET/CT fusion image: The right breast was seen with enlargement, there were multiple soft tissue density masses (green arrow), and there was skin thickening of the right breast with increased metabolism and SUVmax being 3.9. (**d**) Axillary PET/CT fusion image: Multiple enlarged lymph nodes were seen in the right axilla with increased metabolism, which was considered as lymph node metastasis

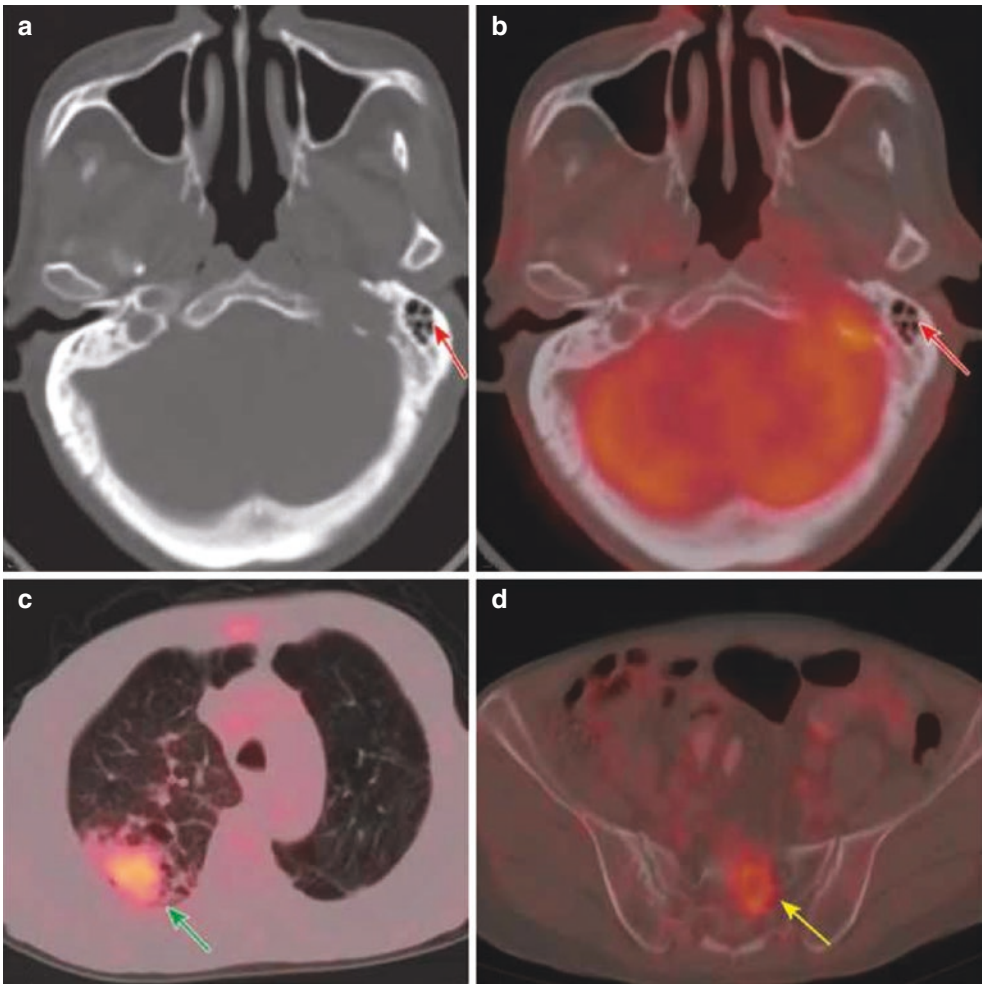

Fig. 16.9 ^{18}F-FDG PET/CT images of petrous metastasis of the temporal bone of lung cancer. (**a** and **b**) CT bone window image and cross section of PET/CT fusion image of the temporal bone, respectively: CT showed osteolysis bone destruction at the petrous part of the left temporal bone (red arrow), which damaged the edge of the lesion in an irregular, worm-biting-like appearance and invaded the jugular vein foramen; PET/CT fusion image showed increased metabolism in the bone destruction lesion, with SUVmax of 3.6. (**c**) Lung PET/CT fusion image: Subpleural differentiation of lobar soft tissue density masses in the upper lobe of the right lung (green arrow), with increased metabolism and SUVmax of about 3.9. (**d**) Sacral PET/CT fusion image: Sacral osteolytic bone destruction with increased metabolism (yellow arrow)

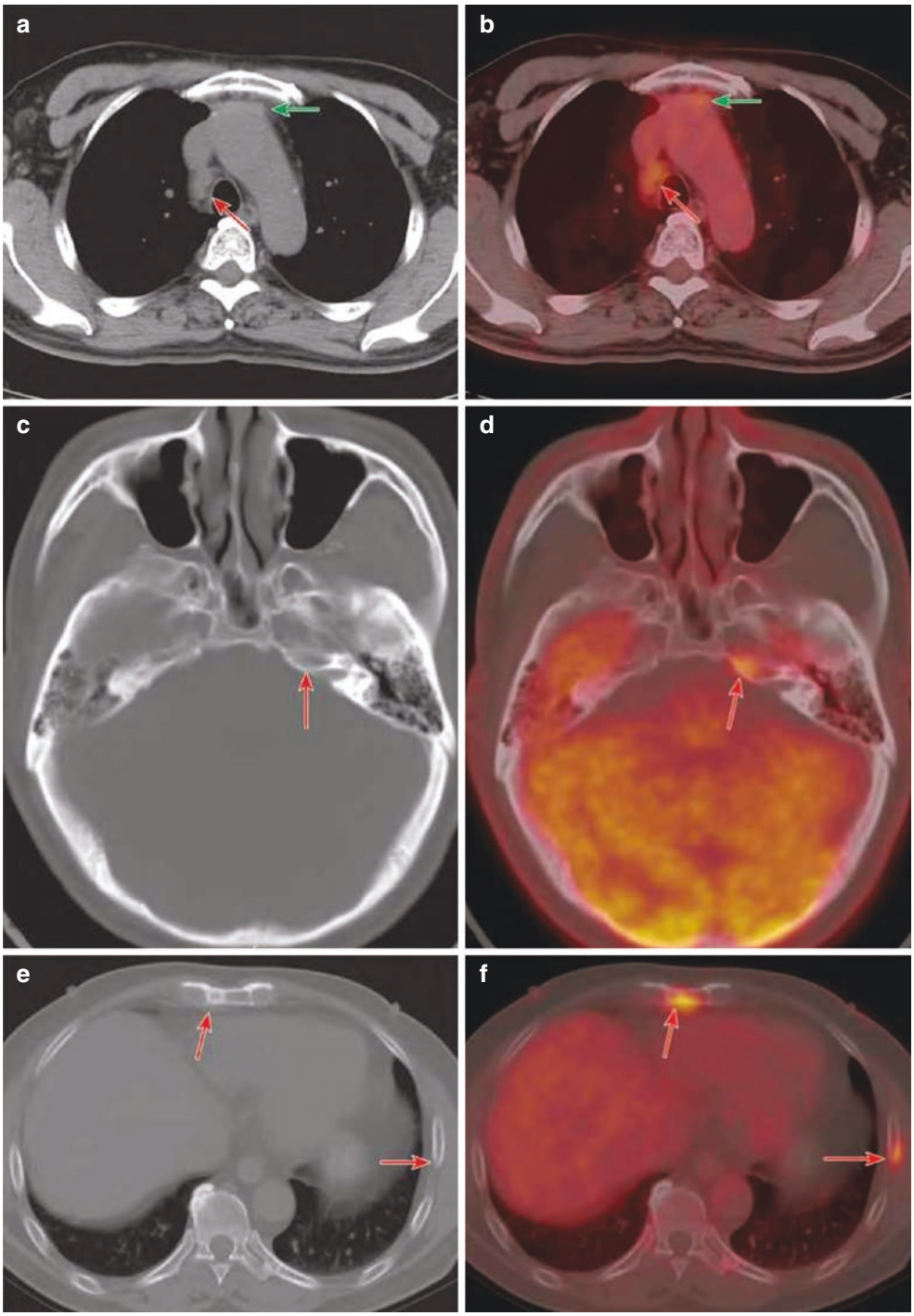

Fig. 16.10 ^{18}F-FDG PET/CT images of postoperative recurrence after surgery for atypical carcinoid tumors of the thymus and metastasis to the petrous part of the temporal bone. Figures **a**, **c**, and **d** were CT images, while Figures **b**, **d**, and **f** were PET/CT fusion images. (**a** and **b**) After thymus operation, local region was seen with irregular soft tissue density lesion (green arrow) and increased metabolism, with SUVmax being about 3.7. Enlarged lymph nodes were discovered (red arrows) in the mediastinum near the right lower trachea with increased metabolism. (**c** and **d**) Focal increased metabolism in the petrous apex of the left temporal bone, with SUVmax 4.3, and no definite bone destruction was found on CT. (**e** and **f**) Sternum osteogenic destruction with increased metabolism and SUVmax 4.9; a focal metabolic increase in the left rib with no confirmable bone destruction. The diagnosis based on PET/CT was recurrence with mediastinal lymph node metastasis and multiple bone metastases. Although lesions with focal increased FDG uptake in the petrous apex of the left temporal bone and left rib showed no definite bone destruction on CT, there were other metastatic lesions out of the head (such as sternal bone metastasis) detected by PET/CT, so it had adequate confidence to identify the focus with increased FDG uptake in the petrous apex of the left temporal bone as a metastatic tumor

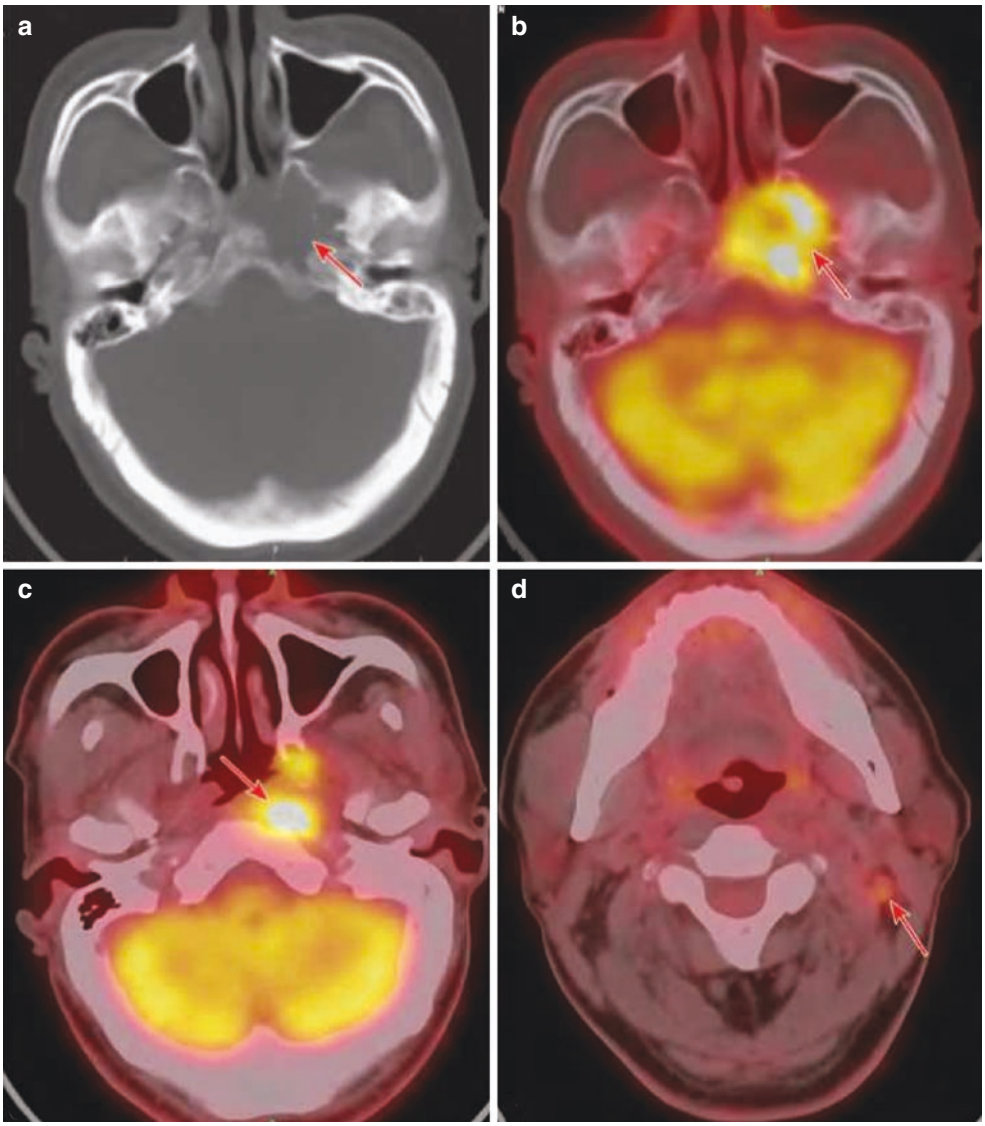

Fig. 16.11 ^{18}F-FDG PET/CT images of nasopharyngeal carcinoma directly invading the petrous apex of the temporal bone. (**a** and **b**) CT bone window image and cross section of PET/CT fusion image of the temporal bone, respectively: CT showed osteolysis bone destruction at the petrous apex of the left temporal bone, basal part of the occipital bone, and greater wing of the left sphenoid bone, soft tissue density lesion was observed, the edge of the destruction area was irregular, and the part was in worm-eaten shape. PET/CT fusion images showed increased focal metabolism in the bone destruction area, and SUVmax was about 11.2. (**c**) PET/CT fusion image at the lower level of Fig. **b**: the left pharyngeal recess became shallow and disappeared, local soft tissue thickened and metabolism increased, SUVmax was about 12.3, and the medial muscle of left wing was invaded. (**d**) Submaxillary plane PET/CT fusion image: lymph node metastasis was seen in the left cervical II region

5.4 Differential Diagnosis

Langerhans cell histiocytosis (LCH):

1. Clinical overview: LCH is a group of tissue-cell proliferative diseases with unknown causes; it is a group of heterogeneous diseases clinically. The pathology is characterized with proliferation of mature eosinophilic cells and Langerhans cells, of which eosinophilic granulomas are the most common. CT image shows osteolytic bone destruction accompanied by soft tissue mass formation, with clear and sharp margins of the destruction lesion, and soft tissue mass shows no invasion to the surrounding bone. In the repair stage, the margin of the damaged lesion may show osteosclerosis, and the range of the late stage sclerosis expands. Osteolytic lesions may contain residual bone fragments, known as "buttonlike dead bones."
2. PET/CT diagnostic points: Most of them are highly metabolized and difficult to distinguish from osteolytic bone metastases. However, PET/CT is used for systemic imaging, and most of them are able to show primary body lesions, which is helpful for the diagnosis of metastatic tumors (Fig. 16.12).

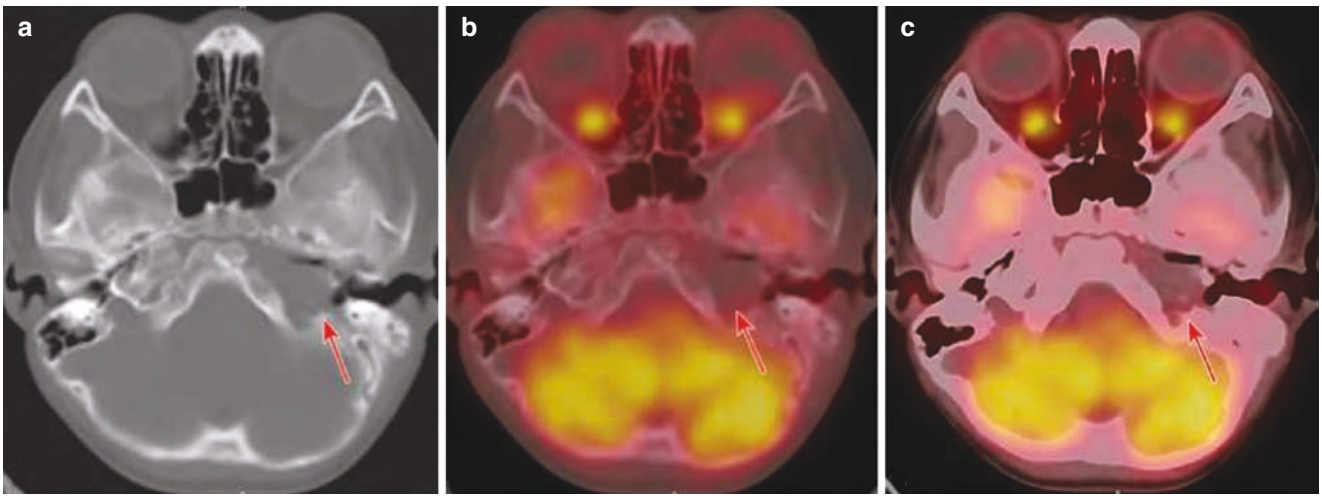

Fig. 16.12 ^{18}F-FDG PET/CT images of Langerhans cell histiocytosis. A 5-year-old child patient with Langerhans cell histiocytosis was reviewed with ^{18}F-FDG PET/CT images after six cycles of chemotherapy: (**a**) CT image (bone window) was seen with osteolytic bone destruction of the petrous part of the left temporal bone and soft tissue density lesion with smooth, sharp margins and no erosion. (**b**) PET/CT fusion image (bone window). (**c**) PET/CT fusion image (soft tissue window). Figures **b** and **c** showed no metabolism in the lesion, while Figures **a** and **c** showed small bone fragments in soft tissue lesions

5.5 Summary

The application value of ^{18}F-FDG PET/CT for temporal bone metastases is higher than that for primary tumors, which is mainly used in:

1. Searching for primary tumors: ^{18}F-FDG PET/CT is helpful for searching for primary tumors in the detection of metastatic tumors or bone destructions in the temporal bone.
2. Understanding the lesion invasion scope: For those inflicted with direct spreading and invasion to the temporal bone, such as nasopharyngeal carcinoma, ^{18}F-FDG PET/CT examination is helpful to determine the local invasion scope and know whether there is local lymph node metastasis or distant metastasis.
3. For patients with known primary lesion, ^{18}F-FDG PET/CT can be used for tumor staging.